Effect of a Monofunctional Phenanthriplatin-DNA Adduct on RNA Polymerase II Transcriptional Fidelity and Translesion Synthesis

Matthew W. Kellinger[1], **Ga Young Park**[2], **Jenny Chong**[1], **Stephen J. Lippard**[2,*], and **Dong Wang**[1,*]

[1]Skaggs School of Pharmacy and Pharmaceutical Sciences, The University of California, San Diego, La Jolla, CA 92093, United States

[2]Department of Chemistry, Massachusetts Institute of Technology, Cambridge, MA 02139, United States

Abstract

Transcription inhibition by platinum anticancer drugs is an important component of their mechanism of action. Phenanthriplatin, a cisplatin derivative containing phenanthridine in place of one of the chloride ligands, forms highly potent monofunctional adducts on DNA having a structure and spectrum of anticancer activity distinct from those of the parent drug. Understanding the functional consequences of DNA damage by phenanthriplatin for the normal functions of RNA polymerase II (Pol II), the major cellular transcription machinery component, is an important step toward elucidating its mechanism of action. In this study, we present the first systematic mechanistic investigation that addresses how a site-specific phenanthriplatin-DNA d(G) monofunctional adduct affects the Pol II elongation and transcriptional fidelity checkpoint steps. Pol II processing of the phenanthriplatin lesion differs significantly from that of the canonical cisplatin DNA 1,2-d(GpG) intrastrand cross-link. A majority of Pol II elongation complexes stall after successful addition of CTP opposite the phenanthriplatin-dG adduct in an error-free manner, with specificity for CTP incorporation being essentially the same as for undamaged dG on the template. A small portion of Pol II undergoes slow, error-prone bypass of the phenanthriplatin-dG lesion, which resembles DNA polymerases that similarly switch from high-fidelity replicative DNA processing (error-free) to low-fidelity translesion DNA synthesis (error-prone) at DNA damage sites. These results provide the first insights into how the Pol II transcription machinery processes the most abundant DNA lesion of the monofunctional phenanthriplatin anticancer drug candidate and enrich our general understanding of Pol II transcription fidelity maintenance, lesion bypass, and transcription-derived mutagenesis. Because of the current interest in monofunctional, DNA-damaging metallodrugs, these results are of likely relevance to a broad spectrum of next-generation anticancer agents being developed by the medicinal inorganic chemistry community.

Introduction

As the first step of gene expression, transcription requires accurate reading of the genetic code from the DNA template strand and faithful synthesis of a complementary messenger

*Corresponding authors: lippard@mit.edu; dongwang@ucsd.edu.

RNA strand by the action of an essential enzyme, RNA polymerase II (Pol II). The fidelity of this process depends not only on the specific patterns of hydrogen bonds between complementary nucleotide base pairs, but also relies on the specific recognition of the template DNA strand and correct selection of NTP substrates by Pol II. DNA-targeted chemotherapeutic drugs alter the chemical and structural properties of the duplex and subsequently modulate transcription and other DNA-dependent cellular processes that lead to the beneficial clinical outcome. Knowledge of the functional interplay between drug-induced DNA modifications and transcription will enhance our understanding of the mechanism of action of these drugs and guide rational improvements in drug design.

The three FDA-approved platinum antitumor drugs, cisplatin (*cis*-diammine-dichloroplatinum(II)), carboplatin (*cis*-diammine(1,1 Ecyclobutanedicarboxylato)-platinum(II)), and oxaliplatin ((*trans-R,R*-diaminocyclohexane)oxalatoplatinum(II)) (Figure 1a),[1–6] form bifunctional platinum-DNA cross-links. The major platinum-DNA adducts are strong roadblocks for Pol II transcription and result in cell death.[7–9] However, recurrence of the disease often occurs as a result of acquired or intrinsic resistance to these platinum-based drugs, owing to repair of the adducts before they can destroy the cancer cell. New platinum-based chemotherapeutics with novel mechanisms of action are needed to overcome these limitations.[1,10–16]

Recently, monofunctional platinum compounds, including pyriplatin (*cis*-diamminepyridinechloroplatinum(II)) and phenanthriplatin (*cis*-diamminephenanthridinechloroplatinum(II)) (Figure 1a), were identified that display a unique spectrum of activity against panels of cancer cell lines. This behavior differentiates them as having a structure-activity relationship distinct from that of cisplatin and its analogs, which form DNA cross-links.[12–15] In contrast to cisplatin, these compounds exclusively form monofunctional adducts, mainly at the N^7 positions of dG and dA deoxynucleotides on the DNA template (Figure 1b).[15] Previously, we reported the structure of Pol II stalled at a pyriplatin-DNA monofunctional adduct.[14] This structure revealed that the adduct introduces a strong steric barrier for Pol II translocation by interacting with the Pol II bridge helix and blocking transition to the next base on the template strand. The mechanism of transcription inhibition by pyriplatin thus differs significantly from that of cisplatin.[14] Transcription inhibition profiles for pyriplatin-DNA adducts were further characterized in a variety of live mammalian cell lines.[16]

To improve the potency of monofunctional Pt(II) complexes, various *N*-heterocyclic ligands (Am) were substituted for pyridine, with guidance from the X-ray structure of Pol II stalled at the pyriplatin-DNA adduct.[14] Among these compounds, phenanthriplatin had the greatest activity, significantly better than that of the three FDA-approved drugs.[15] With the use of globally platinated *Gaussia* luciferase vectors, we determined that transcription is inhibited by phenanthriplatin treatment in live mammalian cells.[15] To gain a deeper mechanistic insight into the action of phenanthriplatin, it is important to determine how specific DNA adducts made by the complex will affect transcription in a defined system using purified RNA Pol II, the enzyme responsible for synthesizing most mRNAs, snRNA, and microRNAs.

Structural and functional studies of RNA Pol II have provided extensive information about how the template DNA and substrate are recognized and subsequently incorporated into the growing RNA chain, as well as how transcriptional fidelity is achieved on undamaged DNA templates.[17–34] The transcriptional fidelity of Pol II is controlled by three checkpoint steps: (1) specific nucleotide selection and incorporation; (2) preferential RNA transcript extension from a matched end; and (3) proofreading by cleavage of the RNA transcript at 3 Eend (Figure 1c).[32] In the first checkpoint step, the nucleotide substrate diffuses into the active

site of RNA Pol II through its secondary channel. If the substrate is matched with the template base, the trigger loop folds into an active closed conformation. The nucleotide addition reaction is greatly facilitated by this closure of the active site.[20] On the other hand, when a mismatched nucleotide is located at the E site, the trigger loop remains in an inactive, open state.[19,20] As a consequence, addition of the mismatched nucleotide is very slow and inefficient. In the second checkpoint step, Pol II can elongate much more efficiently from a matched than a mismatched end, providing a strong kinetic discrimination and opening a time window for the next checkpoint step (Pol II proofreading).[32] Finally, Pol II achieves its proofreading activity by backtracking and preferentially cleaving RNA transcripts that have a mismatched rather than a matched end.[26,32] We recently reported a systematic analysis of the roles that specific hydrogen bonds between base pairs and base stacking play in each of the three fidelity checkpoint steps.[32]

In the present investigation we have dissected the functional interplay between a site-specific phenanthriplatin-DNA dG adduct, the most abundant lesion made by the compound on the duplex, and the Pol II transcription machinery as an important step toward elucidating the mechanism of phenanthriplatin. Although formation of this adduct on the DNA template strand does not directly interfere with G:C Watson-Crick base pairing, it was designed to introduce significant steric hindrance to Pol II on the major groove side of the guanosine base. Here, we present the effect of this adduct on each of the transcriptional fidelity checkpoint steps and report a comprehensive analysis of the functional interplay between the programmed phenanthriplatin-DNA lesion and Pol II transcription.

Experimental Section

Preparation of a DNA Template Containing a Site-Specific Phenanthriplatin dG Adduct

The DNA template containing the site-specific phenanthriplatin-DNA adduct used in transcription assays is as follows:

5 ⎕CTACCCATAACCACCCCG*TCCTCTCCATC -3 ⎕

where G* refers to the phenanthriplatin DNA adduct (Figure 1). The material was prepared and purified by HPLC essentially as described.[15] Detailed procedures for synthesis and characterization are given in the Supporting Information.

Preparation of Pol II Elongation Complex

Saccharomyces cerevisiae yeast Pol II was purified as described.[20,26,31,32] Pol II elongation complexes containing the desired DNA/RNA scaffolds were prepared as described.[20,26,32] Briefly, an aliquot of 5 ⎕[32]P-labeled RNA was annealed with a twofold excess of template and non-template DNA to form an RNA/DNA scaffold in elongation buffer (20 mM Tris-HCl pH 7.5, 40 mM KCl, 5 mM MgCl$_2$). An aliquot of the annealed scaffold was then incubated with a fourfold excess amount of Pol II at room temperature for another 20 min to form Pol II elongation complex for *in vitro* transcription. Scaffolds for the transcription assay are as indicated below (RNA/Template DNA/Non-template DNA):

Scaffold A:

3 ⎕AUGGAGAGGA -5 ⎕

5 ⎕CTACCTCTCCTXCCCCACCAATACCCATC -3 ⎕

3 ⎕GTGGTTATGGGTAG -5 ⎕

X = G or Pt-dG

Scaffold B:

3 □AUGGAGAGGAY -5 □

5 □CTACCTCTCCTXCCCCACCAATACCCATC -3 □

3 □GTGGTTATGGGTAG -5 □

X = G or Pt-dG; Y = C, A, or U

In Vitro Pol II Transcription Elongation Assays

The assay was performed as described.[32] Briefly, aliquots of preformed Pol II elongation complex with scaffold A or B (40 nM) were mixed with equal volumes of elongation buffer containing varied concentrations of ATP, GTP, CTP, UTP, or NTP mixture (final concentrations: 20 □M or 1 mM, respectively). The reactions were incubated for 5 and 60 min at room temperature before quenching with 0.5 M EDTA (pH 8.0). The transcription products were separated by PAGE (15% acrylamide (19:1 bis-acrylamide), 8M urea, 1x TBE) and quantitated with a Molecular Imager PharosFX Plus system (Bio-Rad) and Image Lab software.

Single-Turnover Nucleotide Incorporation Assays

The assay was carried out as previously described.[32] Briefly, nucleotide incorporation was monitored by pre-incubating 100 nM scaffold A or scaffold B with 400 nM Pol II for 20 min in elongation buffer at room temperature (22 °C). The Pol II elongation complex was then mixed with an equal volume of solution containing 40 mM KCl, 20 mM Tris (pH 7.5), 10 mM DTT, 10 mM $MgCl_2$, and various twofold concentrations of CTP (for scaffold A), ATP (for scaffold A), UTP (for scaffold A), or GTP (for scaffold B), respectively. Reactions were quenched at various times by addition of one volume of 0.5 M EDTA (pH 8.0). Reactions requiring time points shorter than 5 s were quenched using a RQF-3 Rapid Quench Flow (KinTek Corp). Products were analyzed by denaturing PAGE as previously described and quantitated with a Molecular Imager PharosFX Plus system (Bio-Rad) and Image Lab software.

Single-Turnover TFIIS-Mediated and Pyrophosphate-Mediated Cleavage Assays

TFIIS-mediated cleavage reactions were performed by pre-incubating Pol II with various scaffolds as previously described.[32] The solutions were then mixed with an equal volume of solution containing 3 □M TFIIS and 10 mM $MgCl_2$. Final reaction conditions were 200 nM Pol II, 50 nM scaffold B, 1.5 □M TFIIS, and 5 mM $MgCl_2$. Reactions were quenched at various time by addition of one volume of 0.5 M EDTA (pH 8.0). Products were separated by denaturing PAGE as previously described. For pyrophosphate-mediated cleavage assays, TFIIS was omitted from the reaction and the Pol II complex was mixed with an equal volume of solution containing 1 mM pyrophosphate.

Data Analysis of Nucleotide Incorporation Kinetics

Data analysis was performed as described.[32] Briefly, the time dependence of transcription product formation at a single concentration of NTP was fit by non-linear regression analysis to an exponential equation using GraFit 5. The NTP concentration dependence of the observed fast rate was then fit to a hyperbolic equation to obtain values for the maximum rate of NTP incorporation (k_{pol}) and a dissociation constant ($K_{d,app}$). The specificity constant (k_{cat}/K_m) was then obtained from $k_{pol}/K_{d,app}$. Discrimination was calculated as the ratio of specificity constants governing two different nucleotide incorporation events defined in the text.

Results

To investigate the effect of a phenanthriplatin monofunctional dG adduct on RNA Pol II transcription elongation bypass and fidelity, we assembled active RNA Pol II elongation complexes with either an undamaged template DNA strand or one containing a site-specific phenanthriplatin-DNA lesion (scaffolds A and B). This *in vitro* system allowed us to directly compare the differences of Pol II transcription along the damaged and undamaged templates. In addition, we could quantitatively measure the effect of the phenanthriplatin-DNA lesion at each checkpoint step of Pol II transcriptional fidelity maintenance.

Effect of a Phenanthriplatin-DNA Lesion on the First Checkpoint Step: Nucleotide Selection and Incorporation

We first investigated whether Pol II is completely blocked by the phenanthriplatin-DNA adduct. When the Pol II elongation complexes were incubated in the presence of 20 or 1000 μM NTP, it was apparent that the transcription elongation patterns differed significantly for undamaged (Figure 2a) versus phenanthriplatin-damaged (Figure 2b) DNA templates. For the undamaged template, the majority of transcripts were longer than 18–20 nt, even at the lower concentration and short time incubation, indicative of efficient transcription elongation (Figure 2a). In contrast, the majority of Pol II transcripts stopped after incorporating one nucleotide (11 nt) on the platinated template (Figure 2b). An additional damage-specific pause site was evident, corresponding to 15 nt (Figure 2b). Only a small amount of bypassed RNA transcript products >15 nt were apparent (Figure 2b).

Because Pol II was able to incorporate at least one nucleotide on the damaged template, we next investigated which substrate is most favored for incorporation opposite to the phenanthriplatin lesion. We incubated Pol II complexes containing either undamaged or damaged template with varied concentrations of ATP, UTP, CTP, or GTP in separate experiments. Intriguingly, we found that the presence of the platinum lesion had little effect on nucleotide selection. For both undamaged and damaged DNA templates, CTP incorporation efficiency is the greatest and GTP the lowest (Figure 2b). In addition, we observed a measureable amount of UTP and ATP misincorportion at prolonged incubation times and higher concentrations (Figure 2b).

Because CTP, ATP, and UTP incorporation opposite the platinum adduct are much more efficient than GTP incorporation, we compared the efficiency of installing these three substrates, CTP being correct but ATP and UTP introducing mutations in RNA transcripts. To provide a quantitative measurement of the effect of the phenanthriplatin-DNA adduct on their first checkpoint step, Pol II nucleotide selection and incorporation, we performed pre-steady-state single turnover transcription assays. The kinetic parameters, k_{pol} (catalytic rate constant) and $K_{d,app}$ (apparent dissociation constant), for CTP, ATP and UTP incorporation were determined using the platinated and unplatinated templates.

As can be seen from Table 1 and Figure 3a, CTP incorporation on the undamaged template yielded values of 760 ± 80 min^{-1}, 91 ± 20 μM, and 8.4 ± 2.0 μM^{-1}min^{-1} for k_{pol}, $K_{d,app}$, and the specificity constant ($k_{pol}/K_{d,app}$), respectively, whereas CTP incorporation on a damaged template resulted in respective values of 17.9 ± 1.5 min^{-1}, 7.2 ± 2.9 μM, and 2.5 ± 1.0 μM^{-1}min^{-1}. Thus the presence of phenanthriplatin generated an ~40-fold decrease in k_{pol} but only an approximately threefold decrease in specificity for CTP incorporation. ATP and UTP misincorporation was significantly slower than CTP incorporation for both damaged and undamaged templates (Table 1 and Figure 3a). Interestingly, there was no significant difference in k_{pol} for misincorporation of ATP and UTP on the platinated compared to the unplatinated template.

Comparison of specificities ($k_{pol}/K_{d,app}$) for CTP and the mismatched nucleotide (ATP or UTP) incorporation provides a quantitative measurement of nucleotide selectivity, or discrimination. We define nucleotide discrimination of CTP over ATP as $(k_{pol}/K_{d,app})_{CTP}/(k_{pol}/K_{d,app})_{ATP}$ and of CTP over UTP as $(k_{pol}/K_{d,app})_{CTP}/(k_{pol}/K_{d,app})_{UTP}$, respectively (Table 2). The CTP/ATP discrimination values are $(1.7 \pm 0.8) \times 10^5$ and $(3.4 \pm 1.4) \times 10^4$ for undamaged and damaged templates, respectively, and for CTP/UTP the respective values are $(3.4 \pm 1.0) \times 10^4$ and $(5.6 \pm 2.7) \times 10^3$. Thus the presence of phenanthriplatin reduces the nucleotide discrimination by only a factor of ~5 (Table 2, Figures 3b and 3c). Taken together, the high nucleotide discrimination in the first checkpoint step is largely maintained even in the presence of the sterically encumbering phenanthriplatin-DNA lesion.

Effect of a Phenanthriplatin-DNA Lesion on the Second Checkpoint Step: Pol II Extension and Bypass

To investigate how the phenanthriplatin-DNA lesion affects the second fidelity checkpoint step, we assembled six Pol II elongation complexes containing a 3′ RNA:DNA terminus: C:dG, A:dG, U:dG, C:Pt-dG, A:Pt-dG, or U:Pt-dG, respectively (scaffold B). Scaffold B contains one more nucleotide at the RNA 3′ end in comparison with scaffold A and mimics three states of the Pol II elongation complex after the first nucleotide incorporation, namely, correct CTP incorporation, ATP misincorporation, and UTP misincorporation, respectively. To test the effect of the 3′ RNA:DNA setting on subsequent nucleotide incorporation, we first incubated the Pol II elongation complexes with varied concentrations of GTP. We observed a significant portion of GTP incorporation on the undamaged template containing a C:dG end, whereas only a small amount of GTP incorporation was observed on the damaged template containing a C:Pt-dG end (Figures 4a and d). Similar differences were observed in the results of prolonged incubation and high concentration of GTP with scaffolds containing A:dG and U:dG versus A:Pt-dG and U:Pt-dG, respectively (Figures 4b, c, and e, f). We further tested the extension ability of these six transcription complexes with a NTP incubation mixture, and we observed that the presence of the DNA lesion significantly reduces the longer transcription products, especially transcripts longer than 15 nt, which are virtually abolished (Figure 4). This result is consistent with the data obtained using scaffold A with a shorter RNA primer.

To quantitatively evaluate the extension kinetics beyond the point of template damage, we next measured the specificity of GTP incorporation with Pol II elongation complexes in scaffolds B, using undamaged templates as controls. This approach allows us to evaluate the influence of both the Pt-DNA adduct and of the different base pairs at the 3′ terminus of the primer on incorporation of the next nucleotide. Intriguingly, we found that replacement of undamaged dG with damaged Pt-dG impacts in a significantly different manner extension from a matched compared with a mismatched pair. The results are summarized in Figures 5 and 6, and Table 3.

Collectively, discrimination of a matched over a mismatched 3′ RNA terminus decreases significantly as a consequence of phenanthriplatin damage on the DNA template. GTP incorporation on the C:dG template is favored by 2,000-fold and 5,000-fold over the A:dG and U:dG mismatch, respectively (Figure 6b). This value decreases significantly with replacement of dG by Pt-dG on the template such that GTP incorporation on the C:Pt-dG scaffold is favored by only ~9-fold and ~14-fold compared with the A:Pt-dG and U:Pt-dG scaffolds, respectively (Figure 6b). Thus, the presence of Pt-DNA lesion significantly slows down incorporation the next nucleotide and greatly diminishes the strong kinetic discrimination of transcript extension from a matched over a mismatched end.

Effect of a Phenanthriplatin-DNA Lesion on the Third Checkpoint Step: Pol II Proofreading of RNA Transcripts

Finally, we investigated the effect of a phenanthriplatin-dG lesion on the third checkpoint step, Pol II proofreading, by performing TFIIS-stimulated cleavage assays using scaffold B in the absence of NTP. The results are presented in Figure 7 and summarized in Table 4. Scaffold B containing a matched 3′ RNA end (C:dG) generates the slowest cleavage rate, whereas template substitution with damaged Pt-dG leads to a 1.6-fold rate increase. For scaffold B containing a mismatched 3′ RNA end (A:dG), the cleavage rate of 12 ± 1 min^{-1} was not significantly changed when template containing damaged Pt-dG was used. For scaffold B containing a mismatched 3′ RNA end (U:dG), the cleavage rate is 8.9 ± 0.3 min^{-1}, and template substitution with damaged Pt-dG leads to only a 1.3-fold decrease in the rate. These results indicate that the fidelity contribution by preferential cleavage of a Pol II complex containing an A:dG mismatched pair over a matched C:dG pair is 17 ± 3 fold, and substitution of a Pt-dG damaged template lowers this value to 13 ± 2 fold. The fidelity contribution by preferential cleavage of a Pol II complex containing a U:dG mismatched pair over a matched C:dG pair is 13 ± 2 fold, and the template substitution with damaged Pt-dG yields a 6 ± 1 fold fidelity contribution.

It is noteworthy that the introduction of Pt-dG did not change the cleavage pattern. The presence of an $n-1$ product (10 nt) and the lack of an $n-2$ product (9 nt) at early time points from C:dG and C:Pt-dG scaffolds indicate the existence of a Pol II pre-translocation state and the absence of a backtracked state. In contrast, the presence of an $n-2$ product (9 nt) and a lack of an $n-1$ product (10 nt) at early time points from A:dG, A:Pt-dG, U:dG, and U:Pt-dG scaffolds suggests the existence of backtracked Pol II and a lack of pre-translocation state (Figure 7). We also performed a pyrophosphate-mediated cleavage assay, which is the reverse reaction of nucleotide addition. This assay cleaves a single 3′ end RNA nucleotide when Pol II is at the pre-translocation state. As shown in Table 5 and Figure 7, we observed similar cleavage rates for the C:dG and C:Pt-dG scaffolds.

Discussion

Effects on Transcriptional Fidelity and Translesion Bypass

Some DNA lesions significantly increase nucleotide misincorporation in RNA transcripts during Pol II transcriptional bypass (error-prone bypass), whereas others have virtually no effect on Pol II fidelity (error-free bypass).[9,35] We systematically investigated the effects of the sterically encumbering, monofunctional platinum-DNA adduct on each of the three checkpoint steps of Pol II transcriptional fidelity and elongation.

The influence of the phenanthriplatin-dG adduct on the template strand is significantly different in each of these three steps. The presence of the monofunctional platinum complex does not prevent efficient CTP incorporation at the first checkpoint, which is strikingly distinct from that of cisplatin and other bifunctional platinum compounds.[2] This result is most likely characteristic of all bulky monofunctional platinum-DNA adducts, for we observed a similar result for a pyriplatin-dG lesion on DNA.[14] The presence of the platinum adduct produces only a threefold decrease in specificity for CTP incorporation, while increasing nucleotide misincorporation by ~1.5- to 1.8-fold. The net result is a minor (fivefold) reduction of nucleotide discrimination in contribution to the total transcriptional fidelity at the first checkpoint step. Thus, Pol II proceeds in an error-free manner at this step and incorporates the correct nucleotide opposite the lesion. CTP incorporation is very accurate, fast, and efficient.

In the second checkpoint step, however, the presence of phenanthriplatin significantly slows transcript extension from a matched dG:C end. The adduct decreases by 500-fold extension

from a matched end, whereas it only causes an approximately twofold decrease in extension from a mismatched end. As a result, the presence of the Pt-dG DNA adduct contributes an ~200- to 500-fold reduction in total transcriptional fidelity at the second checkpoint step. Thus, in the second checkpoint step (extension from the lesion), Pol II transcription is very inaccurate, slow, and inefficient (error-prone). Subsequent G incorporation is greatly inhibited for a damaged versus an undamaged template. There was also a strong pause at the n+1 position, and only a small fraction of Pol II was able to bypass the DNA lesion. In addition, we observed another strong pause site at position n+5 on the damaged template, possibly reflecting an interaction with the switch loop 3 (Rpb2 1118–1127) region of Pol II.[17] This result reveals an additional steric checkpoint upstream (post-nucleotide addition) to monitor possible structural deviation of RNA/DNA duplex due to RNA misincorporation or template DNA damage.

In the third checkpoint step, the presence of the Pt-DNA lesion causes less than a twofold reduction in transcriptional fidelity. Taken together, data obtained from these three checkpoint steps reveal that a phenanthriplatin Pt-DNA dG adduct reduces total transcription fidelity by ~1200–5000-fold. The presence of the phenanthriplatin DNA adduct leads to rapid, "error-free" addition of the first nucleotide opposite the DNA damage site and a slow, "error-prone" addition for subsequent nucleotide extension downstream of the DNA damage site.

Pol II Processing at a Monofunctional Pt-DNA Adduct is Distinct from that at a Bifunctional Cross-link

It is well documented that certain families of DNA polymerases often incorporate dAMP opposite a damaged DNA base in a non-template manner, a phenomenon that is called the "A-rule."[36–43] Although the A-rule holds for certain families of DNA polymerases, it is not a universal feature that applies to all polymerases.[44–46] It was recently reported that Pol II preferentially inserts AMP opposite cisplatin and cyclobutane pyrimidine dimer (CPD) 1,2-intrastrand cross-link lesions.[34] An intriguing question raised by this result is whether the A-rule will apply to other types of lesions. The monofunctional phenanthriplatin-DNA adduct is structurally distinct from adducts of cisplatin and CPD intrastrand cross-links. As summarized in the Results section, Pol II can efficiently incorporate CMP opposite the phenanthriplatin DNA adduct at a rate that is several orders of magnitude higher than that for AMP incorporation. This result differs significantly from that for CPD and cisplatin damage, where incorporation of the correct substrate is significantly reduced by several orders of magnitude. Thus, Pol II does not obey the "A-Rule" (non-template incorporation of AMP opposite DNA damaged bases) at this monofunctional Pt-DNA lesion, indicating that there is no universal mechanism for Pol II bypass of DNA adducts. Rather, Pol II bypass and stalling mechanisms are more likely to be lesion specific. The mechanism of monofunctional adduct bypass is significantly distinct from that of cisplatin intrastrand cross-link, which is substantially more distorted and can be recognized and removed more efficiently by repair enzymes. Monofunctional adducts are therefore more likely to escape direct detection by the nucleotide excision repair machinery. This result could be of more general significance if it applied to monofunctional DNA lesions formed by other metallodrug candidates.

Impact of the Phenanthriplatin-DNA Lesion on Transcription

The presence of DNA damage significantly changes Pol II transcription dynamics with various consequences on transcription including bypass, stalling, and backtracking.[7–9] In particular, prolonged stalling of Pol II at DNA lesions blocks translocation of other important enzymes that progress along the DNA template. Stalled Pol II acts as a strong roadblock for the DNA replication and transcription machinery,[47–49] the collision with

which generates DNA strand breakage and subsequent apoptosis if not repaired. Cells have evolved several strategies to avoid potential stress caused by a stalled Pol II including translesion bypass, transcription-coupled repair, and ubiquitylation leading to proteasome removal.[7,8,50] The present studies establish a platform for extension to other types of DNA damage, particularly that involving other bulky monofunctional adducts. DNA lesions caused by several environmental carcinogens such as benzo[ ]pyrene diol epoxide and acetylaminofluorene can block Pol II transcription.[8,51–53] More detailed comparisons and structural information about the phenanthriplatin-DNA adduct and in complex with the Pol II transcription apparatus would provide a biochemical basis and structural framework for understanding the functional interplay between DNA lesions and transcriptional machinery. This knowledge would also facilitate an understanding of different DNA lesion processing mechanisms caused by chemotherapeutic drugs and environmental carcinogens, which may in turn provide the basis for designing more potent therapeutics.

Conclusion

In summary, we present a systematic mechanistic analysis of the functional interplay between a site-specific phenanthriplatin-DNA monofunctional dG adduct and the Pol II transcription machinery. Whereas a majority of Pol II elongation complexes stall after rapid, error-free addition of CTP opposite the phenanthriplatin-dG adduct, a small portion of Pol II undergoes slow, error-prone bypass of the phenanthriplatin-dG lesion. These results reveal that Pol II processing of the phenanthriplatin lesion is significantly different from that of the canonical cisplatin DNA 1,2-d(GpG) intrastrand cross-link. Furthermore, the influence of the phenanthriplatin-dG adduct on the template strand is significantly different in each of three transcriptional fidelity checkpoint steps. Our studies provide new insights into how the Pol II transcription machinery processes monofunctional phenanthriplatin-DNA adducts. This knowledge establishes a key structure-function relationship that may underlie the strong differentiation in biological consequences between phenanthriplatin and the classical platinum anticancer drugs now widely used in the clinic.

Supplementary Material

Refer to Web version on PubMed Central for supplementary material.

Acknowledgments

References

1. Wang D, Lippard SJ. Nat Rev Drug Discov. 2005; 4:307. [PubMed: 15789122]

2. Todd RC, Lippard SJ. Metallomics. 2009; 1:280. [PubMed: 20046924]

3. Brabec V, Kasparkova J. Drug Resist Updat. 2005; 8:131. [PubMed: 15894512]

4. Reedijk J. Proc Natl Acad Sci USA. 2003; 100:3611. [PubMed: 12655051]

5. Aris SM, Farrell NP. Eur J Inorg Chem. 2009; 2009:1293. [PubMed: 20161688]

6. Kelland L. Nat Rev Cancer. 2007; 7:573. [PubMed: 17625587]

7. Svejstrup JQ. Trends Biochem Sci. 2007; 32:165. [PubMed: 17349792]

8. Hanawalt PC, Spivak G. Nat Rev Mol Cell Biol. 2008; 9:958. [PubMed: 19023283]

9. Saxowsky TT, Doetsch PW. Chem Rev. 2006; 106:474. [PubMed: 16464015]

10. Jamieson ER, Lippard SJ. Chem Rev. 1999; 99:2467. [PubMed: 11749487]

11. Jung YW, Lippard SJ. Chem Rev. 2007; 107:1387. [PubMed: 17455916]

12. Lovejoy KS, Lippard SJ. Dalton Trans. 2009:10651. [PubMed: 20023892]

13. Lovejoy KS, Todd RC, Zhang S, McCormick MS, D'Aquino JA, Reardon JT, Sancar A, Giacomini KM, Lippard SJ. Proc Natl Acad Sci USA. 2008; 105:8902. [PubMed: 18579768]

14. Wang D, Zhu G, Huang X, Lippard SJ. Proc Natl Acad Sci USA. 2010; 107:9584. [PubMed: 20448203]

15. Park GY, Wilson JJ, Song Y, Lippard SJ. Proc Natl Acad Sci USA. 2012; 109:11987. [PubMed: 22773807]

16. Zhu GY, Myint M, Ang WH, Song L, Lippard SJ. Cancer Res. 2012; 72:790. [PubMed: 22180496]

17. Gnatt AL, Cramer P, Fu J, Bushnell DA, Kornberg RD. Science. 2001; 292:1876. [PubMed: 11313499]

18. Kettenberger H, Armache KJ, Cramer P. Mol Cell. 2004; 16:955. [PubMed: 15610738]

19. Westover KD, Bushnell DA, Kornberg RD. Cell. 2004; 119:481. [PubMed: 15537538]

20. Wang D, Bushnell DA, Westover KD, Kaplan CD, Kornberg RD. Cell. 2006; 127:941. [PubMed: 17129781]

21. Brueckner F, Cramer P. Nat Struct Mol Biol. 2008; 15:811. [PubMed: 18552824]

22. Kaplan CD, Larsson KM, Kornberg RD. Mol Cell. 2008; 30:547. [PubMed: 18538653]

23. Kireeva ML, Nedialkov YA, Cremona GH, Purtov YA, Lubkowska L, Malagon F, Burton ZF, Strathern JN, Kashlev M. Mol Cell. 2008; 30:557. [PubMed: 18538654]

24. Sydow JF, Brueckner F, Cheung AC, Damsma GE, Dengl S, Lehmann E, Vassylyev D, Cramer P. Mol Cell. 2009; 34:710. [PubMed: 19560423]

25. Walmacq C, Kireeva ML, Irvin J, Nedialkov Y, Lubkowska L, Malagon F, Strathern JN, Kashlev M. J Biol Chem. 2009; 284:19601. [PubMed: 19439405]

26. Wang D, Bushnell DA, Huang X, Westover KD, Levitt M, Kornberg RD. Science. 2009; 324:1203. [PubMed: 19478184]

27. Huang X, Wang D, Weiss DR, Bushnell DA, Kornberg RD, Levitt M. Proc Natl Acad Sci USA. 2010; 107:15745. [PubMed: 20798057]

28. Cheung AC, Cramer P. Nature. 2011; 471:249. [PubMed: 21346759]

29. Da LT, Wang D, Huang X. J Am Chem Soc. 2012; 134:2399. [PubMed: 22206270]

30. Kaplan CD, Jin H, Zhang IL, Belyanin A. PLoS Genet. 2012; 8:e1002627. [PubMed: 22511879]

31. Kellinger MW, Song CX, Chong J, Lu XY, He C, Wang D. Nat Struct Mol Biol. 2012; 19:831. [PubMed: 22820989]

32. Kellinger MW, Ulrich S, Chong J, Kool ET, Wang D. J Am Chem Soc. 2012; 134:8231. [PubMed: 22509745]

33. Larson MH, Zhou J, Kaplan CD, Palangat M, Kornberg RD, Landick R, Block SM. Proc Natl Acad Sci USA. 2012; 109:6555. [PubMed: 22493230]

34. Walmacq C, Cheung AC, Kireeva ML, Lubkowska L, Ye C, Gotte D, Strathern JN, Carell T, Cramer P, Kashlev M. Mol Cell. 2012; 46:18. [PubMed: 22405652]

35. Tornaletti S, Hanawalt PC. Biochimie. 1999; 81:139. [PubMed: 10214918]

36. Kunkel TA, Schaaper RM, Loeb LA. Biochemistry. 1983; 22:2378. [PubMed: 6344919]

37. Schaaper RM, Kunkel TA, Loeb LA. Proc Natl Acad Sci USA. 1983; 80:487. [PubMed: 6300848]

38. Loeb LA, Preston BD. Annu Rev Genet. 1986; 20:201. [PubMed: 3545059]

39. Strauss BS. Bioessays. 1991; 13:79. [PubMed: 2029269]

40. Goodman MF, Cai H, Bloom LB, Eritja R. Ann NY Acad Sci. 1994; 726:132. [PubMed: 8092671]

41. Strauss BS. DNA Repair. 2002; 1:125. [PubMed: 12509259]

42. Yang W, Woodgate R. Proc Natl Acad Sci USA. 2007; 104:15591. [PubMed: 17898175]

43. Obeid S, Blatter N, Kranaster R, Schnur A, Diederichs K, Welte W, Marx A. EMBO J. 2010; 29:1738. [PubMed: 20400942]

44. Efrati E, Tocco G, Eritja R, Wilson SH, Goodman MF. J Biol Chem. 1997; 272:2559. [PubMed: 8999973]

45. Tang M, Pham P, Shen X, Taylor JS, O'Donnell M, Woodgate R, Goodman MF. Nature. 2000; 404:1014. [PubMed: 10801133]

46. Choi JY, Lim S, Kim EJ, Jo A, Guengerich FP. J Mol Biol. 2010; 404:34. [PubMed: 20888339]

47. Saeki H, Svejstrup JQ. Mol Cell. 2009; 35:191. [PubMed: 19647516]

48. Dutta D, Shatalin K, Epshtein V, Gottesman ME, Nudler E. Cell. 2011; 146:533. [PubMed: 21854980]

49. Hobson DJ, Wei W, Steinmetz LM, Svejstrup JQ. Mol Cell. 2012; 48:365. [PubMed: 23041286]

50. Wilson MD, Harreman M, Svejstrup JQ. Biochim Biophys Acta. 2013; 1829:151. [PubMed: 22960598]

51. Donahue BA, Fuchs RP, Reines D, Hanawalt PC. J Biol Chem. 1996; 271:10588. [PubMed: 8631860]

52. Perlow RA, Broyde S. J Mol Biol. 2002; 322:291. [PubMed: 12217692]

53. Schinecker TM, Perlow RA, Broyde S, Geacintov NE, Scicchitano DA. Nucleic Acids Res. 2003; 31:6004. [PubMed: 14530448]
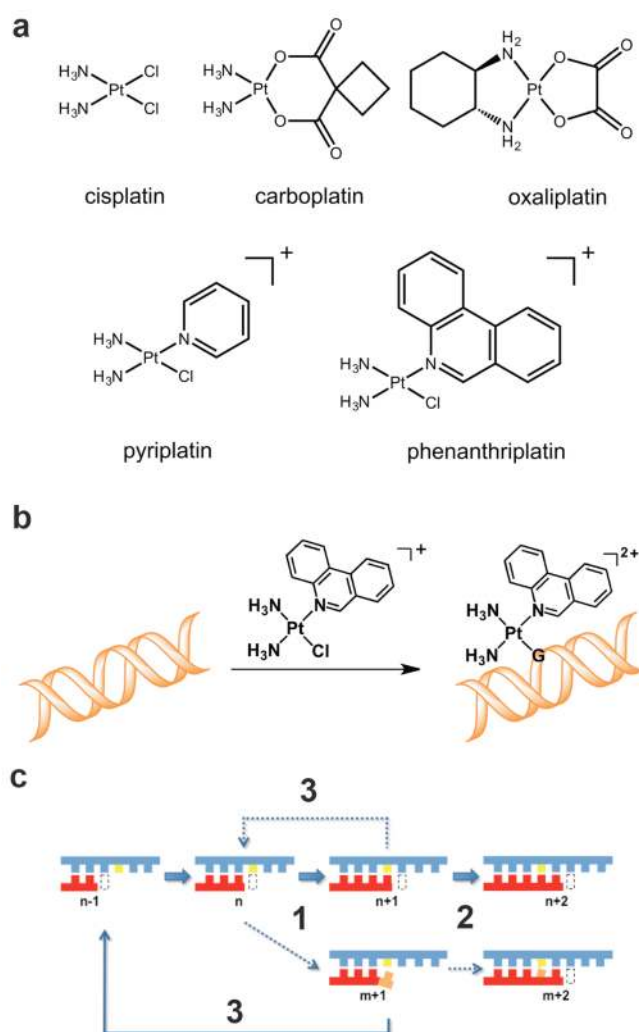
Figure 1.
Monofunctional phenanthriplatin-DNA adduct formation and three key fidelity checkpoint steps of Pol II elongation. (a) Structures of platinum-based anticancer compounds. (b) Phenanthriplatin binds guanosine (G) to form a monofunctional platinum-DNA adduct. Double-stranded DNA is shown in orange. (c) Three key fidelity checkpoint steps of Pol II elongation: (1) nucleotide selection and incorporation, (2) RNA transcript extension, and (3) proofreading. DNA and RNA strands in the Pol II elongation complex are shown in blue and red, respectively. Matched (n) and mismatched (m) nucleotides and their template base are shown in red, orange, and yellow, respectively. Correct and incorrect nucleotide incorporations are depicted with n and m, respectively. The position of the next nucleotide to be added is shown with a dotted box. The widths of the solid lines and arrows correspond to the reaction rates; dotted lines indicate very slow reactions.
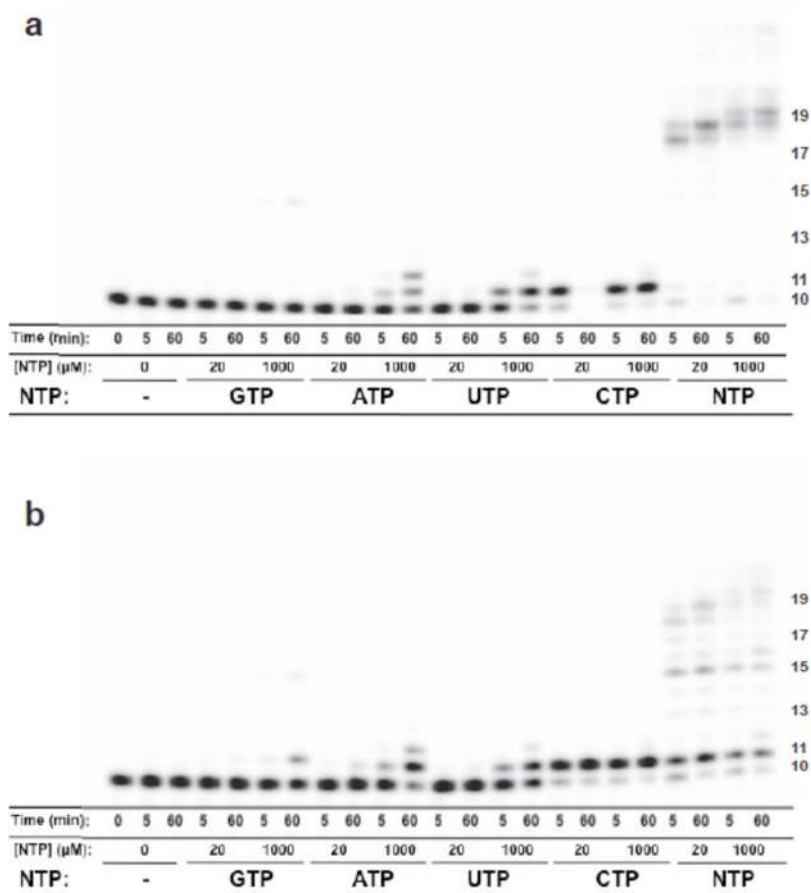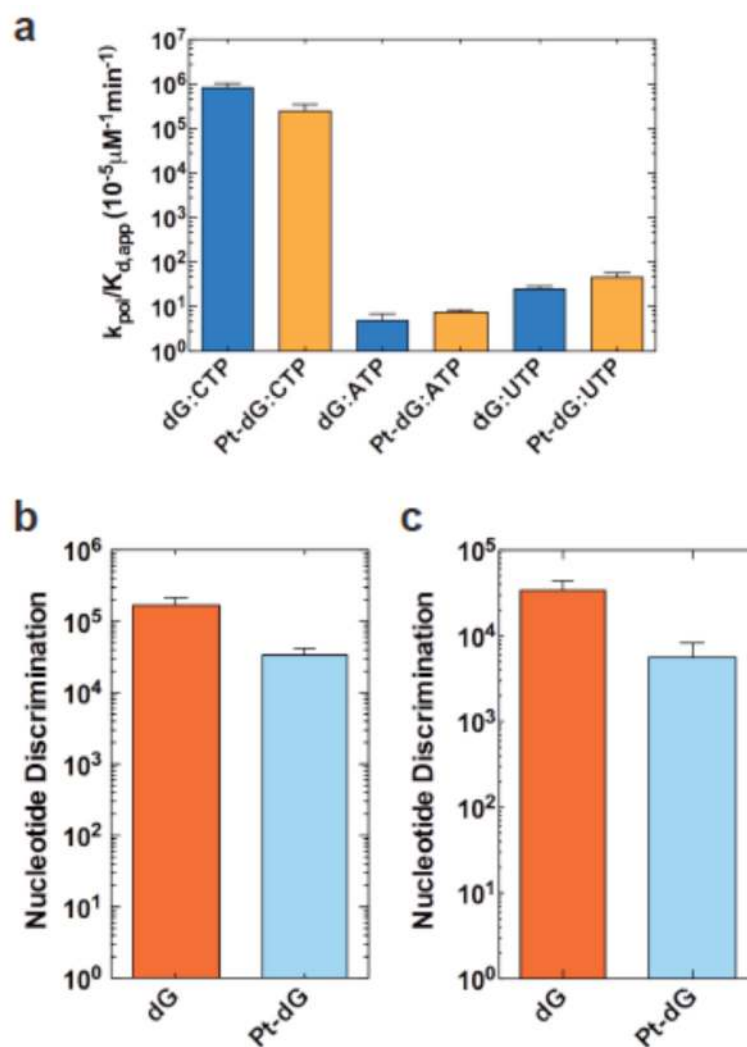
Figure 2.
Phenanthriplatin-DNA adducts substantially block Pol II transcription elongation in comparison to undamaged template. Denaturing PAGE-urea gels of RNA transcripts from (a) an undamaged dG template or (b) a dG template containing site-specific phenanthriplatin damage in the presence of free nucleotide triphosphates.

Figure 3.
Pol II selectively incorporates matched CTP over mismatched ATP or UTP opposite the phenanthriplatin-DNA adduct. (a) The specificity constants governing incorporation (k_{pol}/$K_{d,app}$) of CTP and the mismatched nucleotides ATP and UTP were determined for undamaged template (dG; blue) and phenanthriplatin-damaged template (Pt-dG; orange). Nucleotide discrimination of CTP over the mismatched nucleotides (b) ATP and (c) UTP is defined as $(k_{pol}/K_{d,app})_{CTP}/(k_{pol}/K_{d,app})_{mismatch}$. Nucleotide discrimination was determined for undamaged template (dG; red) and phenanthriplatin-damaged template (Pt-dG; cyan).
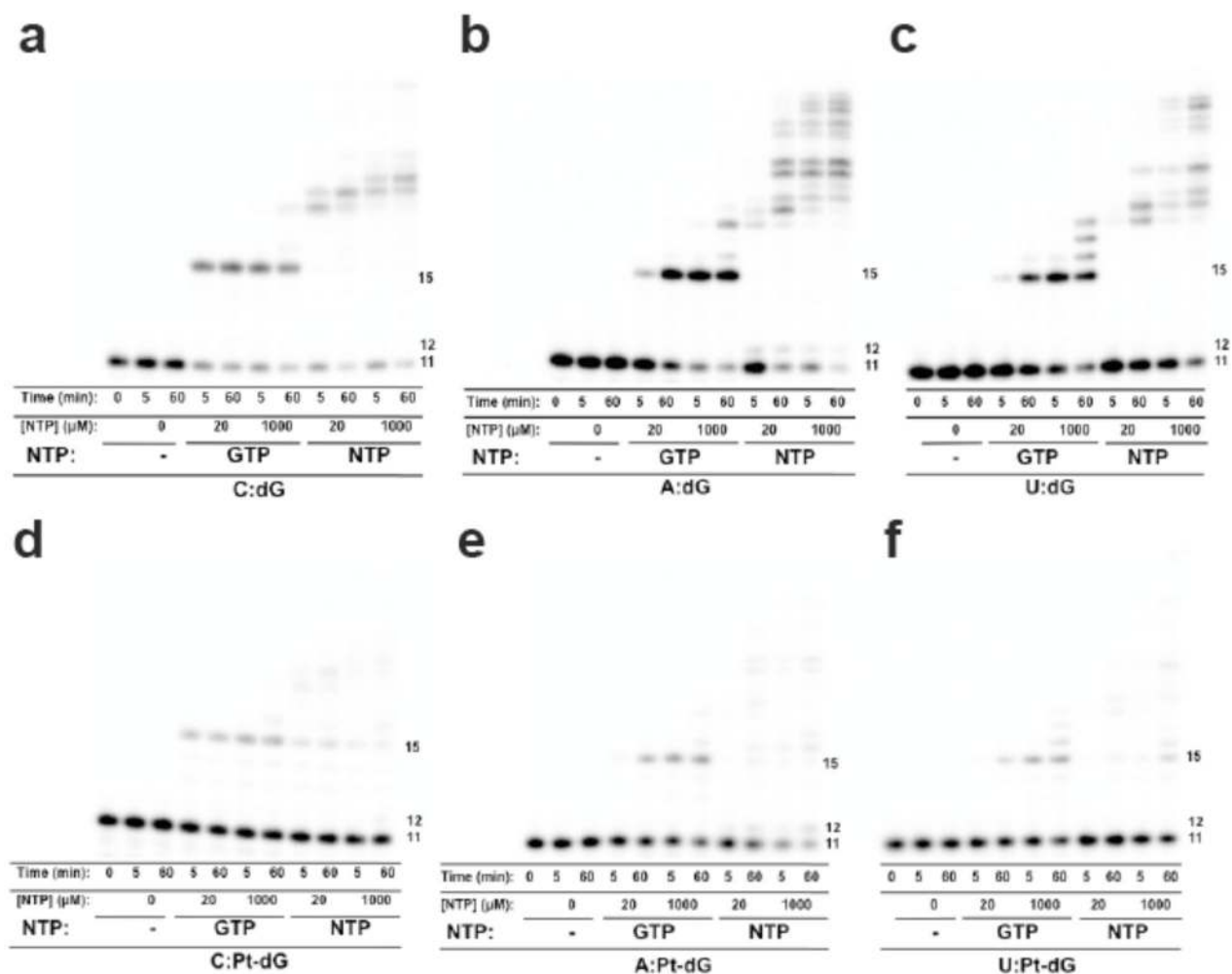
Figure 4.
Nucleotide incorporation and RNA transcript extension by Pol II with undamaged and phenanthriplatin-damaged DNA template. Denaturing PAGE-urea gels of Pol II transcription products from undamaged (dG; a–c) or site-specifically phenanthriplatin-damaged (Pt-dG; d–f) DNA template. ^{32}P-labeled RNA primer (11 nt) was incubated with Pol II, template, and 20 or 1000 μM of GTP or NTP at room temperature for 0, 5, or 60 min; RNA transcripts (≥12 nt) appear as black bands. The 3′ end RNA:DNA base pairs are labeled in (a–f). Only small amounts of bypassed RNA transcript from phenanthriplatin-damaged DNA template were detected following NTP incubation, whereas many more long RNA transcripts (≥15 nt) were observed in the presence of undamaged template.
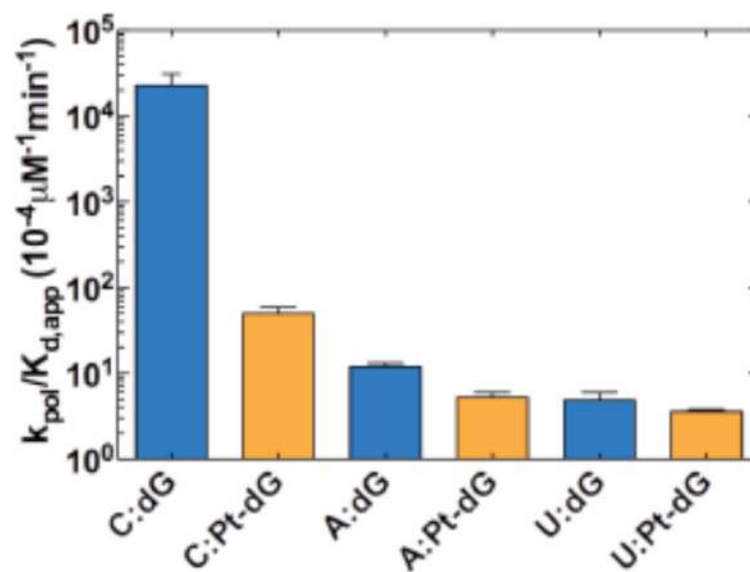
Figure 5.
Phenanthriplatin-DNA adducts substantially reduce the specificity for GTP incorporation from a matched 3′ end. Specificity constants governing GTP incorporation ($k_{pol}/K_{d,app}$) with undamaged (C:dG, A:dG, U:dG; blue) and damaged (C:Pt-dG, A:Pt-dG, U:Pt-dG; orange) templates are depicted.
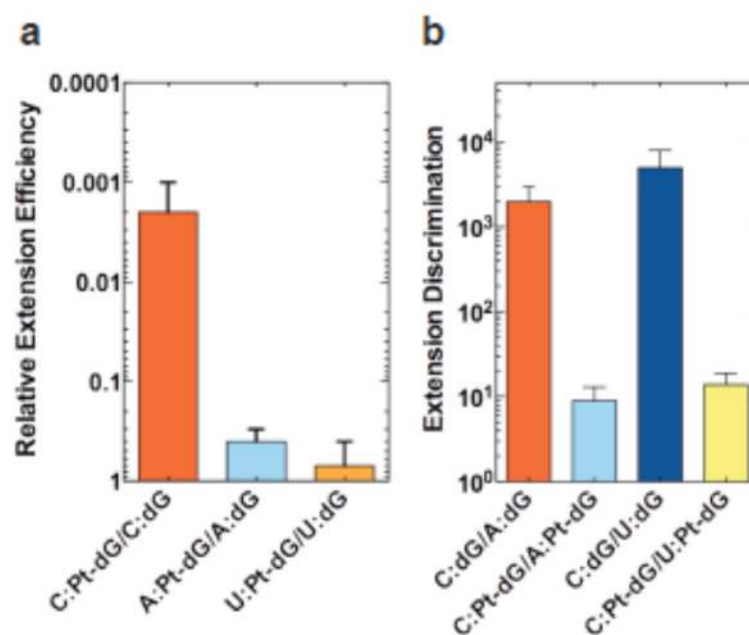
Figure 6.
Phenanthriplatin-DNA adducts substantially decrease the nucleotide extension discrimination in the second checkpoint step. Nucleotide extension discrimination is defined as $(k_{pol}/K_{d,app})_{GTP, \text{matched-end}}/(k_{pol}/K_{d,app})_{GTP, \text{mismatch-end}}$. Undamaged templates are labeled as dG, while damaged templates are labeled as Pt-dG. (a) Relative extension efficiency of C:dG over C:Pt-dG, A:dG over A:Pt-dG, and U:dG over U:Pt-dG are shown in red, cyan, and orange, respectively. Relative extension efficiency is defined by the ratio of $(k_{pol}/K_{d,app})_{GTP}$ for the phenanthriplatin-damaged template to $(k_{pol}/K_{d,app})_{GTP}$ for the undamaged template. (b) Nucleotide extension discrimination of C:dG over A:dG, C:Pt-dG over A:Pt-dG, C:dG over U:dG, and C:Pt-dG over U:Pt-dG are shown in red, cyan, blue, and yellow, respectively.
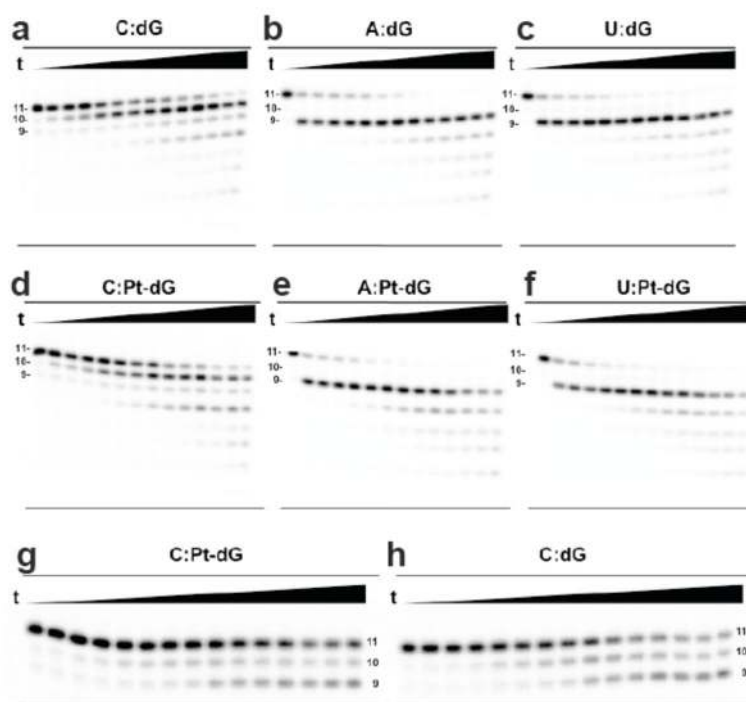
Figure 7.
Phenanthriplatin-DNA adducts do not change Pol II proofreading activity in the third step. TFIIS-mediated RNA transcript cleavage from scaffolds containing a pair of (a) C:dG, (b) A:dG, (c) U:dG, (d) C:Pt-dG, (e) A:Pt-dG, or (f) U:Pt-dG at the 3′ RNA terminus was determined. Pyrophosphate-mediated RNA transcript cleavage was also measured from scaffolds containing (g) C:dG or (h) C:Pt-dG at the 3′ RNA terminus. In each panel, incubation time increases from left to right up to 3 h.

Table 1

Nucleotide Incorporation Opposite Undamaged vs Phenanthriplatin-Damaged Templates

Template Base	NTP	k_{pol} (min^{-1})	$K_{d,app}$ (μM)	$k_{pol}/K_{d,app}$ (M^{-1}min^{-1})	Fold Change[a]
dG	CTP	760 ± 80	91 ± 20	8.4 ± 2.0	0.3 ± 0.1
Pt-dG	CTP	17.9 ± 1.5	7.2 ± 2.9	2.5 ± 1.0	
dG	ATP	0.096 ± 0.015	1950 ± 710	$(4.9 \pm 2.0) \times 10^{-5}$	1.5 ± 0.6
Pt-dG	ATP	0.084 ± 0.004	1130 ± 150	$(7.4 \pm 1.0) \times 10^{-5}$	
dG	UTP	0.34 ± 0.02	1350 ± 170	$(2.5 \pm 0.4) \times 10^{-4}$	1.8 ± 0.6
Pt-dG	UTP	0.32 ± 0.03	710 ± 190	$(4.5 \pm 1.3) \times 10^{-4}$	

[a]Fold Change = ($k_{pol}/K_{d,app}$)Pt-dG/($k_{pol}/K_{d,app}$)dG

Table 2

Nucleotide Discrimination Opposite Undamaged vs Phenanthriplatin-Damaged Templates

Template Base	Discrimination of CTP over ATP[a]	Discrimination of CTP over UTP[b]
dG	$(1.7 \pm 0.8) \times 10^5$	$(3.4 \pm 1.0) \times 10^4$
Pt-dG	$(3.4 \pm 1.4) \times 10^4$	$(5.6 \pm 2.7) \times 10^3$
Change in Discrimination[c]	0.20 ± 0.12	0.17 ± 0.09

[a] Discrimination of CTP over ATP = $(k_{pol}/K_{d,app})CTP/(k_{pol}/K_{d,app})ATP$

[b] Discrimination of CTP over UTP = $(k_{pol}/K_{d,app})CTP/(k_{pol}/K_{d,app})UTP$

[c] Change in Discrimination = $(Discrimination)_{Pt-dG}/(Discrimination)_{dG}$

Table 3

Kinetics of Subsequent Nucleotide Extension on Undamaged *vs* Phenan-thriplatin-Damaged Templates

3′ Terminal Base Pair	k_{pol} (min⁻¹)	$K_{d,app}$ (μM)	$k_{pol}/K_{d,app}$ [a] (μM⁻¹min⁻¹)	Relative Extension Efficiency	
				Template Modification[b]	3′ RNA Mismatch[c]
C:dG	180 ± 30	78 ± 45	2.3 ± 1.4	$(2 ± 1) × 10^{-3}$	1
A:dG	3.0 ± 0.2	2500 ± 400	$(1.2 ± 0.2) × 10^{-3}$	0.4 ± 0.1	$(2 ± 1) × 10^{3}$
U:dG	2.5 ± 0.5	5100 ± 1700	$(4.9 ± 1.9) × 10^{-4}$	0.7 ± 0.3	$(5 ± 3) × 10^{3}$
C:Pt-dG	1.00 ± 0.08	200 ± 60	$(5.0 ± 1.6) × 10^{-3}$	-	1
A:Pt-dG	0.31 ± 0.02	580 ± 130	$(5.3 ± 1.2) × 10^{-4}$	-	9 ± 4
U:Pt-dG	0.36 ± 0.01	990 ± 90	$(3.6 ± 0.3) × 10^{-4}$	-	14 ± 5

[a] Specificity constant = $k_{pol}/K_{d,app}$

[b] Template Modification Relative Extension Efficiency = $(k_{pol}/K_{d,app})$X:Pt-dG/$(k_{pol}/K_{d,app})$X:dG X=A or U

[c] 3′ RNA Mismatch Relative Extension Efficiency = $(k_{pol}/K_{d,app})$C:dG/$(k_{pol}/K_{d,app})$X:dG or $(k_{pol}/K_{d,app})$C:Pt-dG/$(k_{pol}/K_{d,app})$X:Pt-dG, X=A or U

Table 4

Effect of Phenanthriplatin-DNA Lesion on TFIIS-Mediated Cleavage

Template	3′ RNA Nu-cleotide	Cleavage Rate (min^{-1})	Fidelity Contribution[a]	Fidelity Change[b]
dG	C	0.7 ± 0.1	-	-
Pt-dG	C	1.1 ± 0.2	-	-
dG	A	12 ± 1	17 ± 3	-
Pt-dG	A	14 ± 1	13 ± 2	0.8 ± 0.2
dG	U	8.9 ± 0.3	13 ± 2	-
Pt-dG	U	7.1 ± 0.7	6 ± 1	0.5 ± 0.1

[a]Fidelity Contribution = (k$_{TFIIS}$)X:Y/(k$_{TFIIS}$)C:Y X=A or U; Y=dG or Pt-dG

[b]Fidelity Change = (k$_{TFIIS}$)Pt-dG/(k$_{TFIIS}$)dG

Table 5

Effect of Phenanthriplatin-DNA Lesion on Pyrophosphate-Mediated Cleavage

Template	3′ RNA Nucleotide	Cleavage Rate (min⁻¹)
dG	C	$(3.8 \pm 0.3) \times 10^{-2}$
Pt-dG	C	$(3.1 \pm 0.3) \times 10^{-2}$